Letter

Precision comagnetometry for T-violation searches in crystals

Bassam Nima,[1] Mingyu Fan,[1] Aleksandar Radak,[1] Andrew M. Jayich,[2] and Amar Vutha[1]
[1]*Department of Physics, University of Toronto, Toronto, Ontario, Canada M5S 1A7*
[2]*Department of Physics, University of California - Santa Barbara, Santa Barbara, California 93106, USA*

(Received 22 December 2024; revised 21 July 2025; accepted 22 August 2025; published 11 September 2025)

Searches for time-reversal symmetry (T) violations using spin sensors are susceptible to spurious frequency shifts and noise from magnetic fields, which can mask signals originating from beyond-standard-model new physics. Therefore, a comagnetometer—an auxiliary sensor that allows mundane magnetic-field effects to be differentiated from new physics—is an essential feature of many precision measurements. We characterize an intrinsic comagnetometer that is available in crystals, which can be used to suppress spurious magnetic-field effects through comparing sets of ions related by spatial reflection symmetry. We find that the new-physics measurement channel can be effectively shielded to better than 10 μG, without the need for active or passive magnetic shields. Our measurements demonstrate precise and accurate control over magnetic systematic errors, laying the groundwork for improved searches of T violation using solid-state systems.

DOI: 10.1103/jykv-rsd1

The inconsistencies between the standard model of particle physics and astrophysical evidence, such as dark matter and the dominance of matter over antimatter in the universe, motivate searches for new particles or interactions that break time-reversal symmetry (T) [1]. For instance, static T violation produced by new particles or forces generically lead to nonzero electric dipole moments of fundamental particles [2]. Axionlike dark matter models postulate new fields that lead to oscillatory T violation in nuclear interactions [3].

Precision measurements searching for T violation in laboratory experiments typically rely on measurements of energy differences between spin states, whether in particles such as neutrons [4], atoms [5], or polar molecules [6,7]. However, the spins of these systems are always associated with magnetic moments, which makes such experiments susceptible to magnetic fields: fluctuating magnetic fields add noise and degrade the precision of spin sensors, whereas magnetic fields correlated with changes in experiment parameters can introduce systematic errors. Therefore, a strategy commonly employed in such precision measurements is to use a different spin system as a comagnetometer, in order to track magnetic-field changes and distinguish their effects from genuine new physics [8].

Comagnetometer techniques used in searches for new physics range from the use of an entirely different species (e.g., Hg as a comagnetometer in neutron electric dipole moment searches [4]) to the use of different internal states within the same system (e.g., parity doublets states in searches for the electron electric dipole moment with polar molecules [7,9]). Unsurprisingly, any fluctuations in the magnetic moment of the comagnetometer species compared to the system of interest, or variations in their spatial distributions, introduce ways for residual systematic errors to enter into precision measurements [8].

A nuclear T-violation search can be performed using spectroscopy of rare-earth ions in solids, in order to take advantage of the significantly larger number of trapped polarized atoms that are available in doped crystals compared to traditional beams or laser-cooled atomic and molecular experiments. While rare-earth-doped crystals with highly coherent optical transitions have been employed for quantum information storage [10,11] and laser frequency stabilization [12,13], they can also be used to explore the parameter space of new physics occurring at extreme energy scales (>100 TeV). In Refs. [14,15], methods were proposed for performing T-violation searches using non-centrosymmetric crystals containing octupolar rare-earth nuclei, such as ^{153}Eu, which are expected to be highly sensitive to new physics. When rare-earth ions are in non-centrosymmetric sites in crystals, they are strongly electrically polarized by the local fields produced by neighboring ions: these polarized ions produce measurable frequency shifts due to T-violating nuclear moments and they also offer convenient features for mitigating noise and systematic errors. In particular, different groups of ions in these crystals can be used as comagnetometers to control magnetic-field effects in T-violation search experiments, as we demonstrate in this Letter.

The essential idea behind comagnetometry in such crystals is to use mirror-symmetric sets of ions that have identical magnetic properties but opposite T-violation sensitivities. In spirit and intent, our work follows the experiments of Royce and Bloembergen [16], who used oppositely polarized Cr^{3+} ions in crystals to set one of the earliest experimental bounds on T violation. Here we show that this basic idea can be extended and applied to crystals containing octupolar nuclei, resulting in comagnetometers that can accurately track and cancel magnetic-field fluctuations in a system that has enhanced sensitivity to T violation.

Our experiments use $^{153}Eu^{3+}$ ions doped into yttrium orthosilicate (YSO). The crystal structure of YSO (space group C_2/c) is shown in Fig. 1. The locations of the ions within the primitive cell for Y_2SiO_5 are obtained from the Materials Project database [17]. Each primitive cell contains four "site 1" locations where Eu^{3+} ions can be situated. Ions in

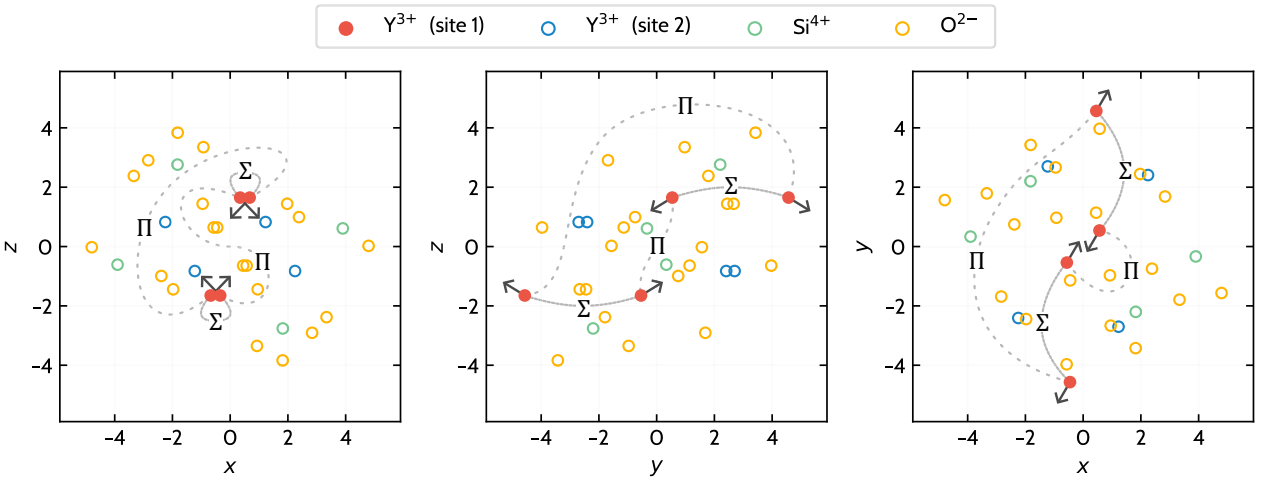

FIG. 1. Crystal structure of a YSO primitive cell, viewed from three orthogonal directions. The x, y, z axes correspond to the dielectric $D1, D2, b$ axes in angstrom units. Each "site 1" Y^{3+} is plotted with an arrow corresponding to the projected direction of the nearest O^{2-} site (some of which are outside of the shown primitive cell). The arrows aid in the visualization of the $\hat{\Sigma}$ or $\hat{\Pi}$ transformation of the Y^{3+} local environments; $\hat{\Sigma}$ is a 180° rotation around the z axis and $\hat{\Pi}$ is a parity flip.

site 1 (where the wavelength of the ${}^7F_0 - {}^5D_0$ transition is 580.04 nm) are shown as filled circles in the figure. In the following, we use x, y, z to refer to the $D1, D2, b$ dielectric axes of the crystal for convenience of notation and we restrict our attention to "site 1" ions in YSO [18]. Primitive cells in the YSO crystal contain four equivalent Y^{3+} ion positions where Eu^{3+} can be substituted. There are two symmetries relating these positions. The first is a reflection through the origin,

$$\hat{\Pi} : (x, y, z) \to (-x, -y, -z). \tag{1}$$

The second is a 180° rotation around the z axis,

$$\hat{\Sigma} : (x, y, z) \to (-x, -y, z). \tag{2}$$

These transformations are illustrated in Fig. 1.

Consequently, the Hamiltonians for Eu^{3+} ions at these four positions are related to one another. Using the symbols $\pi = \pm 1$ and $\sigma = \pm 1$ to label the ion positions according to the irreducible representation of the $\hat{\Pi}$ and $\hat{\Sigma}$ symmetries, respectively, the effective Hamiltonians for the nuclear spin degree of freedom at the four positions, in a particular electronic state of the ion, are

$$H(\sigma, \pi) = \sum_{i,j} Q_{ij} I_i I_j - \sigma\,(\mu_x \mathcal{B}_x + \mu_y \mathcal{B}_y) - \mu_z \mathcal{B}_z - \sigma\pi D\hat{n} \cdot \vec{\mathcal{E}}\,\mathbb{I} + \pi\,\Omega\,\hat{I} \cdot \hat{n}. \tag{3}$$

The indices $i, j = 1$ to 3 label the cartesian axes and $\vec{\mathcal{E}}$ and $\vec{\mathcal{B}}$ are respectively the electric and magnetic fields applied to the Eu:YSO crystal. The nuclear spin is $\vec{I}$, the electric quadrupole moment tensor is Q_{ij}, and $\mu_i = -\sum_j M_{ij} I_j$ are the magnetic-moment components in terms of the gyromagnetic tensor M_{ij} [19]. The quantity $\vec{D} = D\hat{n}$ is the electric dipole moment of the polarized Eu^{3+} ion, with $\mathbb{I}$ being the identity operator in the nuclear spin state space. The $-\sigma\pi D\hat{n} \cdot \vec{\mathcal{E}}\,\mathbb{I}$ term is a common-mode energy shift for all the nuclear spin sublevels in an electronic state of the ion, with a sign that depends on the ion's electric polarization. The quantity Ω parametrizes the energy shift due to a possible nonzero P-odd, T-odd nuclear moment that is produced by beyond-standard-model T violation.

From the Hamiltonians in Eq. (3), it is evident that ions related by the $\hat{\Pi}$ transformation have identical quadrupole and Zeeman shifts, but their opposite electrical polarization—due to their oppositely oriented local environments—endows them with opposite sensitivity to the Ω term. By taking advantage of rf-optical double resonance, nuclear spin transitions in ions with different values of π can be separately read out using Stark shifts of their optical transitions (due to the $\sigma\pi D\hat{n} \cdot \vec{\mathcal{E}}\,\mathbb{I}$ term). In contrast, nuclear spin transitions in ions with different values of σ have different resonance frequencies when the magnetic field is applied, e.g., along the x and z directions (due to the $\sigma\mu_x\mathcal{B}_x + \mu_z\mathcal{B}_z$ term), but they have identical shifts due to electric fields. As we show below, these two types of behavior can be used to isolate the π-dependent Ω term, which contains information about possible beyond-standard-model physics, and separate it from spurious magnetic-field effects.

Crucially, all these measurements can be made just by changing optical and rf frequencies, without requiring mechanical or electrical switches that could introduce correlated systematic errors. The $\sigma = \pm 1, \pi = \pm 1$ ensembles of Eu^{3+} ions therefore act as accurate mutual comagnetometers. In the following, we show that such a scheme can be experimentally implemented and practically used in precision measurements.

The energy-level structure of Eu:YSO is shown in Fig. 3. The 580 nm optical transition connects the ground ${}^7F_0$ electronic state to the excited ${}^5D_0$ electronic state in Eu^{3+}. The quadrupole interaction splits the six nuclear spin sublevels into three sets of state pairs related by Kramers degeneracy [19]. In a crystal such as YSO where there is no spherical symmetry to the environment of an ion, angular momentum quantum numbers are not useful labels for the eigenstates of the nuclear-spin Hamiltonian. So instead, we use letters to label the states and bars over the letters

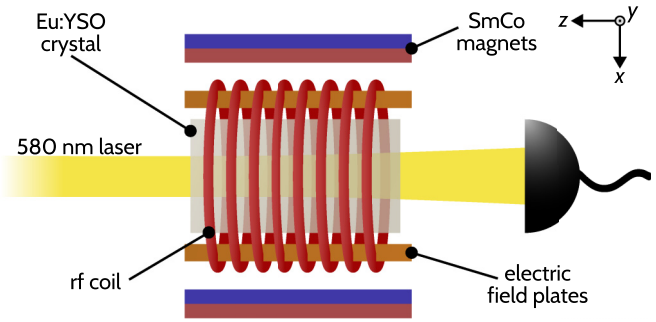

FIG. 2. Schematic diagram of the apparatus. The rf frequency measurements in Figs. 5 and 6 were made using laser absorption spectroscopy of the $^7F_0 - {}^5D_0$ transition in a Eu:YSO crystal at 5 K. The crystal was placed between a pair of electric-field plates, contained within rf coils. SmCo permanent magnets were used to apply a static magnetic field parallel to the electric field.

to denote Kramers conjugates. Thus the eigenstates of the quadrupole interaction are labeled $\bar{a}, a; \bar{b}, b; \bar{c}, c$ in the $^7F_0$ electronic state and $\bar{a}', a'; \bar{b}', b'; \bar{c}', c'$ in the $^5D_0$ electronic state.

The T-violation sensitivities of the $\bar{a}, a; \bar{b}, b; \bar{c}, c$ states are discussed in Ref. [15]. For the measurements reported here, we focus on the $b \to \bar{b}$ transition. The resonance frequency of this transition has magnetic-field sensitivity $\partial f(b,\bar{b})/\partial \mathcal{B}_x \approx 0.6$ kHz/G. Therefore, without comagnetometry and using magnetic-field control alone, it is challenging to measure resonance frequency shifts due to beyond-standard-model T violation that are expected to be $\lesssim 1$ mHz.

The YSO crystal in our experiments is doped with $^{153}Eu^{3+}$ at a concentration of 0.01% and has dimensions 3.5 mm × 4.0 mm × 5.0 mm. The crystal was mounted in a cryocooler and held at approximately 5 K. A schematic of the apparatus

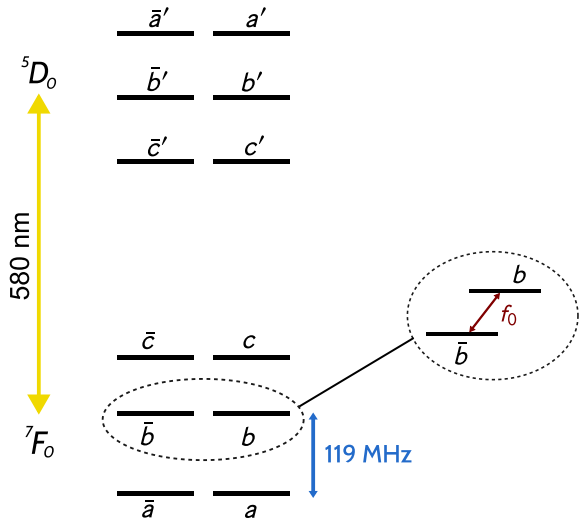

FIG. 3. Energy levels of $^{153}Eu^{3+}$:YSO. The ground $^7F_0$ and excited $^5D_0$ electronic states are connected by a 580 nm optical transition. In the measurements reported here, the $b - \bar{b}$ nuclear spin transition was probed using rf spectroscopy. The energy difference f_0 depends mainly on the applied magnetic field, along with a small contribution due to possible T violation in the ^{153}Eu nucleus.

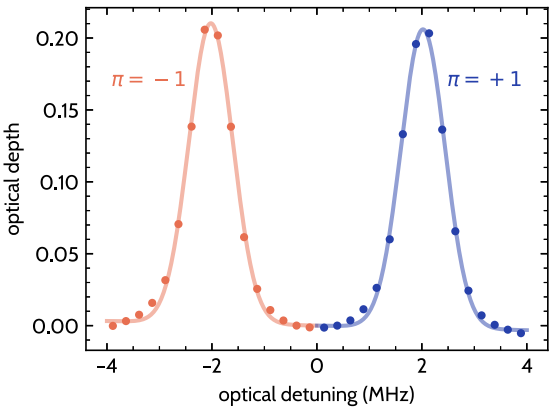

FIG. 4. Optical spectrum with $\mathcal{E}_{dc} \approx 70$ V/cm, used to resolve the $\pi = \pm 1$ ensembles. The optical depth is proportional to the population in the $a, \bar{a}$ hyperfine states. Here optical depth (OD) is related to the laser power measured before the crystal (P_i) and after transmission through the crystal (P_t) as OD $= -\ln(P_t/P_i)$.

is shown in Fig. 2. A pair of silver-coated plates adjacent to the crystal were used to apply an electric field $\mathcal{E}_{dc} = 70$ V/cm along the $\hat{x}$ axis, which shifts the optical absorption resonances from the $\pi = \pm 1$ ensembles by $\Delta\nu_{\mathcal{E}} = \pm 2$ MHz, as shown in Fig. 4. A solenoid around the crystal and field plates was used to generate high-frequency rf magnetic fields at 119 MHz along the $\hat{z}$ axis in order to drive the $a, \bar{a} \to b, \bar{b}$ transition in the $^7F_0$ ground electronic state, for state preparation and detection. A pair of coils aligned along the $\hat{x}$ axis were used to apply low-frequency (∼200 kHz) rf fields to drive the $b \to \bar{b}$ transition for spectroscopy. Samarium-cobalt permanent magnets were used to apply a static magnetic field, $\mathcal{B}_x \approx 350$ G, across the Eu:YSO crystal: we chose this value of $\mathcal{B}_x$ in order to resolve the $a \to b$ and $\bar{a} \to \bar{b}$ resonances on the 119 MHz transition. External coils were used to apply a small static magnetic field $\mathcal{B}_z \approx 7$ G to resolve the $\sigma = \pm 1$ ensembles, shifting their resonances by $\Delta f_0 = \pm 3$ kHz, as shown in Fig. 5. There is no magnetic shielding around the apparatus. The lifetime of the excited $^5D_0$ electronic state is

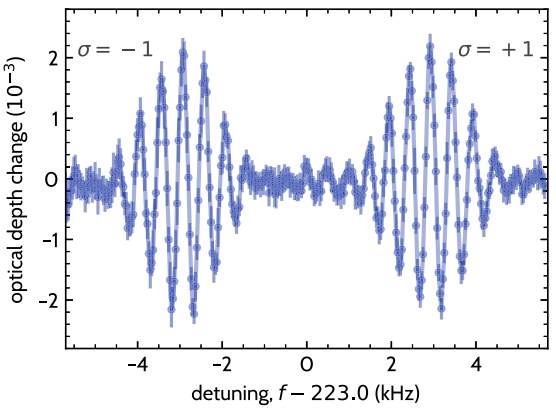

FIG. 5. Example Ramsey spectrum of the $b - \bar{b}$ transition for the $\sigma = \pm 1, \pi = +1$ ensembles, using $\tau = 20$ μs and $T = 80$ μs. Eu^{3+} ions were initially prepared in the b state using optical pumping and the transition probability was measured using laser absorption, while scanning the carrier frequency of the Ramsey pulses.

approximately 1.9 ms and the lifetime (T_1) for the nuclear spin levels within the $^7F_0$ manifold exceeds one day, at the temperatures used in the experiment [20]. Therefore, it is necessary to prepare the states used for measurements using lasers and rf fields. With the $\mathcal{E}$ field on, we used optical and rf pulses to initialize the ^{153}Eu ions into a single nuclear spin state. A sequence of laser pulses were used to drive the $^7F_0\ a, \bar{a} \rightarrow {}^5D_0\ c', \bar{c}'$ and $^7F_0\ c, \bar{c} \rightarrow {}^5D_0\ b', \bar{b}'$ transitions, while rf pulses drove the 119 MHz $\bar{b} \rightarrow \bar{a}$ transition within the ground $^7F_0$ electronic state. The state-preparation sequence follows the method used in Ref. [21], with the only difference being a final $\bar{b} \rightarrow \bar{a}$ rf pulse to prepare ions in the b state.

Following state preparation, the $\mathcal{E}$ field was switched off and rf spectroscopy of the $b \rightarrow \bar{b}$ transition was performed using the Ramsey method [22]. Two pulses of duration τ separated by an interval T were applied to the crystal and the carrier frequency of these pulses was varied. To obtain good signal-to-noise ratio, the measurement of the resonance frequency f_0 for the $b \rightarrow \bar{b}$ transition was repeated with six different choices of relative phases (between 0° and 180°) between the Ramsey pulses. The population excited by the rf spectroscopy pulses to the $\bar{b}$ state was subsequently transferred to the a state using an adiabatic sweep pulse (swept from 40 kHz below the $\bar{b} \rightarrow a$ resonance to 40 kHz above it in 12 ms). After this transfer the population in the a state was measured using optical absorption on the $^7F_0\ a, \bar{a} \rightarrow {}^5D_0\ c', \bar{c}'$ transition.

Since the state-preparation step is performed in the presence of an $\mathcal{E}$ field, two resolved optical absorption lines corresponding to the $\pi = \pm 1$ ensembles can be observed on the $^7F_0\ a, \bar{a} \rightarrow {}^5D_0\ c', \bar{c}'$ transition, as shown in Fig. 4. Measurement of the optical depth of these absorption lines, as the carrier frequency of the spectroscopy pulses is scanned across the $b \rightarrow \bar{b}$ transition, yields two resonance frequencies $f_0(\sigma = \pm 1, \pi)$ for each value of π as shown in Fig. 5. We define $f_c = f_0(\pi = +1) + f_0(\pi = -1)$ the common-mode frequency and $f_d = f_0(\pi = +1) - f_0(\pi = -1)$ the difference frequency. Genuine T-violation signals from new physics sources ought only to appear in f_d, whereas magnetic-field effects that are common to both sets of comagnetometer ions are contained in f_c.

In order to test the accuracy of comagnetometry in this system, we continuously monitored the resonance frequencies for the $\sigma = -1$, $\pi = \pm 1$ ensembles over the course of 10 h. Slow variations of magnetic fields—slower than a frequency measurement cycle time (∼0.5 s), but faster than the period of $\mathcal{E}$-field switches (100–1000 s)—constitute the main backgrounds during precision searches for T violation. To quantitatively test the rejection of magnetic fields in this band, we simultaneously applied sinusoidal magnetic-field perturbations along the three coordinate axes, at a different frequency along each axis ($f_x = 3$ mHz, $f_y = 7$ mHz, and $f_z = 11$ mHz) for ease of analysis. The magnetic-field amplitudes ($\mathcal{B}_{x,0} = 7.15$ mG, $\mathcal{B}_{y,0} = 14.9$ mG, and $\mathcal{B}_{z,0} = 13.5$ mG) were adjusted to create 10-Hz-amplitude oscillations in f_c. As can be seen in Fig. 6, the applied magnetic-field modulation is easily measured in f_c, but it is undetectable in the f_d time series. Note that we have subtracted the average values from the time series for f_c and f_d in Fig. 6 to clearly show the time-varying perturbations. We fit a sum of three sinusoids at the known modulation frequencies to the f_c and f_d time series and for each axis $i = x, y, z$ we define the rejection ratio R_i as the ratio of the fitted modulation amplitudes in f_d and f_c. We find $R_x = (0 \pm 6) \times 10^{-4}$, $R_y = (4 \pm 6) \times 10^{-4}$, and $R_z = (2 \pm 6) \times 10^{-4}$. Equivalently, the magnetic field is canceled to $\delta|\mathcal{B}| \leqslant 9$ μG. These measurements confirm that the $\pi = \pm 1$ ensembles track each other exceptionally well.

Thus our measurements have verified that oppositely polarized Eu^{3+} ions in Eu:YSO have identical magnetic moments to better than one part per thousand. Oppositely polarized ions in the crystal—related by reflection symmetry—act as excellent mutual comagnetometers, with no detectable leakage of magnetic-field effects into the T-violation search channel.

Importantly, whereas the comagnetometer ions have identical shifts due to magnetic fields, they have *opposite* sensitivities to T-violating new physics, as can be seen from the π dependence of the Ω term in Eq. (3). Thus errors and noise due to magnetic fields, which lead to common-mode frequency shifts of the comagnetometer ions, can be cleanly distinguished from the differential shifts produced by T-violating new physics. We anticipate that systematic error control with the rejection ratio demonstrated here—particularly in combination with laboratory electric-field reversals to reject other sources of systematic errors—can be used to make a measurement of the new physics parameter Ω to better than 1 mHz, which would lead to useful bounds on new physics models [15]. The methods demonstrated in this paper are widely applicable for improving the accuracy of other precision measurements, such as dark matter searches, using solid-state systems.

In summary, we have performed comagnetometry using the nuclear spins of mirror-symmetric ions in a crystal, demonstrating that shifts in their nuclear-spin transitions due to magnetic fields can be accurately canceled. Our work shows that *in situ* comparison between sets of ions related by spatial symmetries is a powerful means to advance the precision and accuracy of searches for T violation beyond the standard model.

We thank Y. Takahashi, J. Weinstein, E. Hessels, and P. Goldner for helpful discussions. H. Ramachandran, J. Ford, and D. Stedman contributed to the development of an early version of the apparatus. We are grateful to B. Amos and P. Woitalla for vital technical support. M.F. acknowledges funding from a CQIQC Postdoctoral Fellowship and A.R. acknowledges funding from a CQIQC Undergraduate Summer Research Award. A.M.J. acknowledges the support of the Gordon and Betty Moore Foundation [Grant DOI: 10.37807/gbmf12970]. This project was enabled by support from the John Templeton Foundation (Grant No. 63119), the Alfred P. Sloan Foundation (Grant No. G-2023-21045), and NSERC (Grant No. SAPIN-2021-00025).

The data that support the findings of this article are openly available [23].

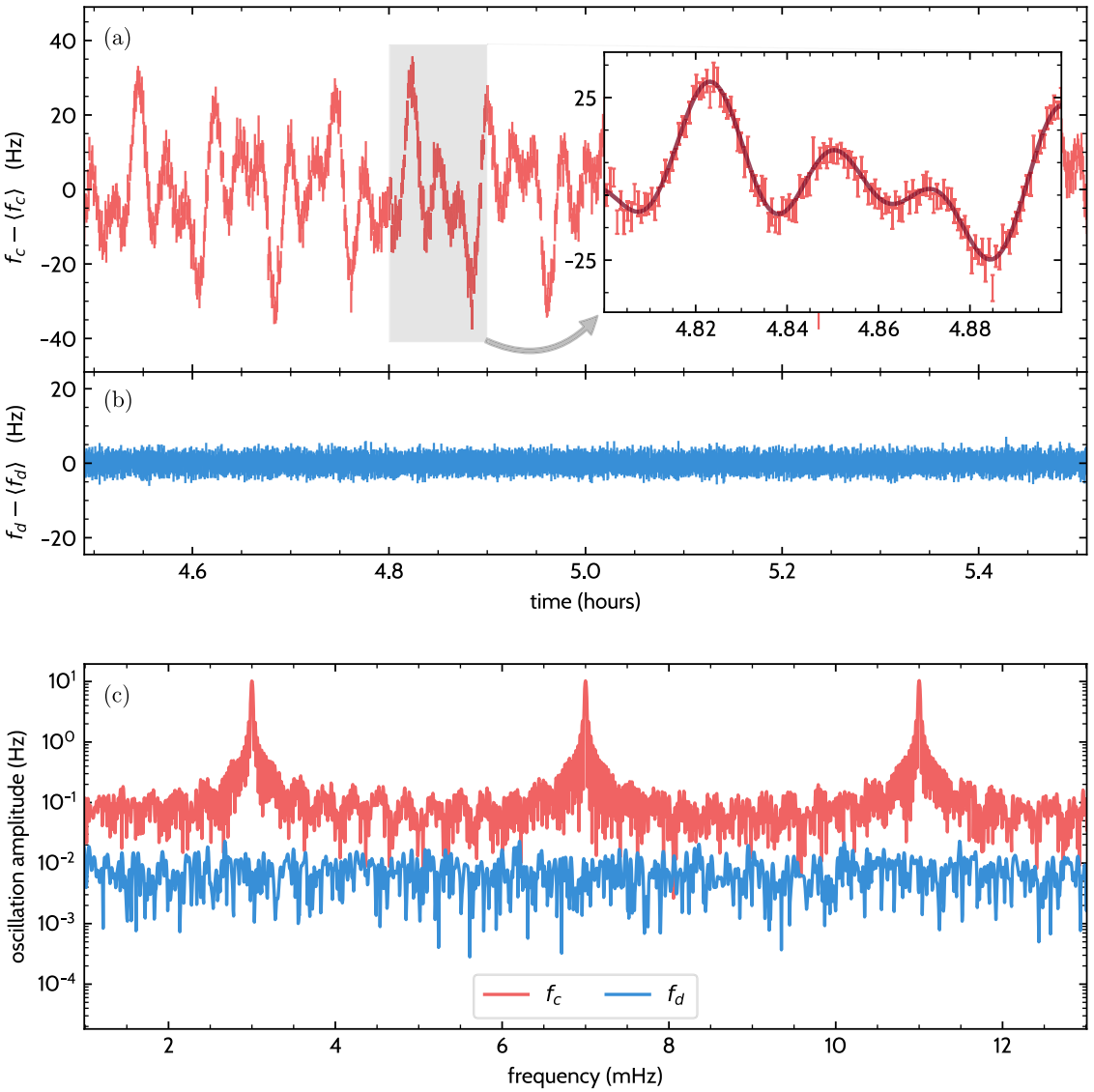

FIG. 6. (a) One-hour-long subset of the measured f_c time series, with its average subtracted. The inset shows the fitted sinusoids, whose amplitudes for the f_c channel are $a_x = 10.29(3)$ Hz, $a_y = 10.23(3)$ Hz, and $a_z = 10.38(3)$ Hz. (b) The f_d time series over the same time span, with its average subtracted. (c) Noise spectrum of the full 10-hour-long f_c and f_d time series. Frequency shifts due to intentionally applied magnetic fields at $f_x = 3$ mHz, $f_y = 7$ mHz, and $f_z = 11$ mHz are evident in the common-mode channel (f_c), but are undetectable in the differential channel (f_d).

[1] W. B. Cairncross and J. Ye, Atoms and molecules in the search for time-reversal symmetry violation, Nat. Rev. Phys. **1**, 510 (2019).

[2] I. B. Khriplovich and S. K. Lamoreaux, *CP Violation Without Strangeness: Electric Dipole Moments of Particles, Atoms, and Molecules* (Springer, Berlin, 2012).

[3] F. Chadha-Day, J. Ellis, and D. J. Marsh, Axion dark matter: What is it and why now? Sci. Adv. **8**, eabj3618 (2022).

[4] C. Abel *et al.*, Measurement of the permanent electric dipole moment of the neutron, Phys. Rev. Lett. **124**, 081803 (2020).

[5] B. Graner, Y. Chen, E. G. Lindahl, and B. R. Heckel, Reduced limit on the permanent electric dipole moment of ^{199}Hg, Phys. Rev. Lett. **116**, 161601 (2016).

[6] ACME Collaboration, Improved limit on the electric dipole moment of the electron, Nature (London) **562**, 355 (2018).

[7] T. S. Roussy, L. Caldwell, T. Wright, W. B. Cairncross, Y. Shagam, K. B. Ng, N. Schlossberger, S. Y. Park, A. Wang, J. Ye, and E. A. Cornell, An improved bound on the electron's electric dipole moment, Science **381**, 46 (2023).

[8] W. A. Terrano and M. V. Romalis, Comagnetometer probes of dark matter and new physics, Quantum Sci. Technol. **7**, 014001 (2022).

[9] D. DeMille, F. Bay, S. Bickman, D. Kawall, L. Hunter, D. Krause, S. Maxwell, and K. Ulmer, Search for the electric dipole moment of the electron using metastable PbO, AIP Conf. Proc. **596**, 72 (2001).

[10] A. Ortu, A. Holzäpfel, J. Etesse, and M. Afzelius, Storage of photonic time-bin qubits for up to 20 ms in a rare-earth doped crystal, npj Quantum Inf. **8**, 29 (2022).

[11] R. Oswald, M. G. Hansen, E. Wiens, A. Y. Nevsky, and S. Schiller, Characteristics of long-lived persistent spectral holes in Eu^{3+}:Y_2SiO_5 At 1.2 K, Phys. Rev. A **98**, 062516 (2018).

[12] Q.-F. Chen, A. Troshyn, I. Ernsting, S. Kayser, S. Vasilyev, A. Nevsky, and S. Schiller, Spectrally narrow, long-term stable optical frequency reference based on a Eu^{3+} : Y_2SiO_5 crystal at cryogenic temperature, Phys. Rev. Lett. **107**, 223202 (2011).

[13] S. Cook, T. Rosenband, and D. R. Leibrandt, Laser-frequency stabilization based on steady-state spectral-hole burning in Eu^{3+} : Y_2SiO_5, Phys. Rev. Lett. **114**, 253902 (2015).

[14] H. D. Ramachandran and A. C. Vutha, Nuclear T-violation search using octupolar nuclei in a crystal, in *The 27th International Conference on Atomic Physics* (Cambridge University Press, Cambridge, UK, 2022).

[15] H. D. Ramachandran and A. C. Vutha, Nuclear T-violation search using octopole-deformed nuclei in a crystal, Phys. Rev. A **108**, 012819 (2023).

[16] E. B. Royce and N. Bloembergen, Linear electric shifts in the paramagnetic resonance of Al_2O_3: Cr and MgO: Cr, Phys. Rev. **131**, 1912 (1963).

[17] The Materials Project, Materials data on Y_2SiO_5 by materials project, retrieved from database version v2025.06.09, DOI:10.17188/1206949.

[18] R. Yano, M. Mitsunaga, and N. Uesugi, Ultralong optical dephasing time in Eu^{3+} : Y_2SiO_5, Opt. Lett. **16**, 1884 (1991).

[19] J. J. Longdell, A. L. Alexander, and M. J. Sellars, Characterization of the hyperfine interaction in europium-doped yttrium orthosilicate and europium chloride hexahydrate, Phys. Rev. B **74**, 195101 (2006).

[20] F. Könz, Y. Sun, C. W. Thiel, R. L. Cone, R. W. Equall, R. L. Hutcheson, and R. M. Macfarlane, Temperature and concentration dependence of optical dephasing, spectral-hole lifetime, and anisotropic absorption in Eu^{3+}:Y_2SiO_5, Phys. Rev. B **68**, 085109 (2003).

[21] E. Z. Cruzeiro, J. Etesse, A. Tiranov, P.-A. Bourdel, F. Fröwis, P. Goldner, N. Gisin, and M. Afzelius, Characterization of the hyperfine interaction of the excited $^5D_0$ state of Eu^{3+} : Y_2SiO_5, Phys. Rev. B **97**, 094416 (2018).

[22] N. F. Ramsey, A molecular beam resonance method with separated oscillating fields, Phys. Rev. **78**, 695 (1950).

[23] B. Nima, Comagnetometry with Eu:YSO, Zenodo, 2025, https://doi.org/10.5281/zenodo.16927434.